PHOTONICS Research

Photonic two-particle quantum walks in Su–Schrieffer–Heeger lattices

Friederike Klauck, Matthias Heinrich, and Alexander Szameit*

Institute for Physics, University of Rostock, 18059 Rostock, Germany
**Corresponding author: alexander.szameit@uni-rostock.de*

Received 1 September 2020; revised 30 October 2020; accepted 14 November 2020; posted 18 November 2020 (Doc. ID 409005); published 24 December 2020

We report on the experimental demonstration of two-photon quantum walks at the edge of a photonic Su–Schrieffer–Heeger lattice and compare them to those observed when launching photons at the edge of a homogeneous lattice. Whereas at the topological edge, one of the photons primarily remains close to the edge, both photons penetrate freely from the trivial edge into the bulk. This behavior manifests also in the average interparticle distance, which is significantly larger at the topological edge. Hence, for a given propagation length, the entangled two-photon state launched at the topological edge extends over a wider domain of the lattice.

https://doi.org/10.1364/PRJ.409005

1. INTRODUCTION

Topological photonics promises unique and robust designs for novel photonic functionalities by rendering device performance immune to degradation induced by fabrication imperfections or environmental changes [1,2]. Topological notions in photonics are inspired by condensed matter physics, and in particular the foundational concept of topological insulators [3–6]. This novel phase of matter is insulating in the bulk, yet conveys surface currents without any dissipation or backscattering, even in the presence of defects and disorder. In 2008, the key features of the electronic quantum Hall effect were adapted to light waves in the proposal of a photonic analogue of the anomalous quantum Hall effect [7,8]. These groundbreaking ideas were first implemented in photonic crystals for the microwave regime [9,10], where topological propagation of microwaves along the edge of the system was demonstrated to form a scatter-free channel.

This demonstration of robust light transport along the edge of a photonic system proved the concept of unidirectional waveguiding based on topology. The first implementation of a photonic topological insulator employed helical waveguides in a honeycomb geometry [11] and was soon followed by a realization based on coupled resonator optical waveguides [12]. Subsequently, numerous peculiar topological phenomena such as anomalous topological insulators [13,14], 4D topological Hall physics [15], Weyl points [16], topological Anderson insulators [17], topological insulators in synthetic dimensions [18], as well as non-Hermitian topological physics [19,20] and topological quantum physics [21,22], were observed and reported.

The majority of one-dimensional systems realized with static waveguide arrays are based on the Su–Schrieffer–Heeger (SSH) model [23], since it is the only topologically nontrivial system in 1D where the time reversal operator squares to one [24]. As expressed in the bulk-edge correspondence, the topology of the lattice interior determines whether topological edge states can exist at the system's boundary. In photonics, such edge states were experimentally realized for the first time in the form of Shockley surface states [25]. SSH lattices were explored in the context of high harmonic generation [26], periodic driving in Floquet systems [27,28], and soliton states [29]. Yet another concept utilizes the framework of optical supersymmetry transformations [30] to connect different SSH-type lattices [31], which triggers topological phase transitions. Also, the SSH model is often used to study the impact of non-Hermitian concepts on topology [19,20].

More recently, the evolution of quantum states in photonic topological systems began to attract considerable interest [21], with a particular emphasis on preserving the quantum coherence due to topological protection [12,22,32–36]. Coupled waveguide lattices have proven to be an exceptionally versatile platform for exploring the evolution of photonic quantum states in complex settings within the framework of photonic quantum walks [37,38]. Beyond the average photon number in the individual channels, i.e., the expectation value of the photon number distribution, an important measure for the quantum behavior of multiphoton states in waveguide lattices is higher-order correlations, which relate to the joint probabilities of finding the photons at particular locations [39–45]. These correlations generally become highly nontrivial for

indistinguishable photons as soon as several paths lead to the same average photon number in the channels, as quantum path interference occurs.

In our work, we experimentally demonstrate two-photon quantum correlations in an SSH waveguide lattice. We explore the specific features of such correlations for the topological as well as the trivial edge and compare them to the homogeneous case. Moreover, we evaluate the inter-particle distance for both edges and find that the topological edge gives rise to larger average distances compared to the trivial edge.

2. THEORETICAL FRAMEWORK

The SSH model describes a one-dimensional lattice of alternatingly coupled sites; see Fig. 1(A). With the coupling constants c_1 and c_2, we define the dimerization $d = \frac{c_1 - c_2}{c_1}$ as a measure for the coupling contrast, such that $d = 0$ corresponds to the homogenous lattice. The evolution of light in these systems can be described using the one-particle time-dependent Schrödinger equation with the Hamiltonian [19,23]

$$H = \begin{pmatrix} 0 & c_1 & 0 & \cdots & 0 \\ c_1 & 0 & c_2 & & \vdots \\ 0 & c_2 & 0 & c_1 & 0 \\ \vdots & & c_1 & 0 & \vdots \\ 0 & \cdots & 0 & \cdots & 0 \end{pmatrix}. \tag{1}$$

For an infinite chain, the Bloch Hamiltonian can be written in k-space as

$$H(k) = \begin{pmatrix} 0 & c_1 + c_2 e^{ik} \\ c_1 + c_2 e^{-ik} & 0 \end{pmatrix}, \tag{2}$$

which results in the dispersion relation [46]

$$E(k) = \pm\sqrt{c_1^2 + c_2^2 + 2c_1 c_2 \cos k} \tag{3}$$

depicted in the band structure in Fig. 1(B). For a homogenous chain (dimerization $d = 0$), the bands intersect, while any nonzero dimerization opens up a band gap. The natural topological invariant of the system is the winding number $W = \frac{Z}{\pi}$, with the Zak phase

$$Z = i \int_{BZ} \psi^*(k) \frac{\partial}{\partial k} \psi(k) \partial k, \tag{4}$$

where $\psi(k)$ is an eigenstate in k-space. For finite lattices, the reversal of couplings is nontrivial [47], and it changes the waveguide of the unit cell that terminates the lattice. In this vein, the bulk–boundary correspondence gives rise to a topological edge state of zero energy where the lattice terminates with weak coupling, where the winding number is $W = 1$, leading to the band structure shown in Fig. 1(C). If the lattice instead terminates at the strong coupling (trivial edge), the winding number is zero and no edge state is supported.

To describe the evolution of quantized light, the single-photon Hamiltonian for a coupled waveguide array reads [48]

$$H = \frac{\hbar c}{n_0} \sum_k \left[\beta_0 \left(\hat{a}_k^\dagger \hat{a}_k + \frac{1}{2} \right) + \sum_l C_{k,l} \hat{a}_k^\dagger \hat{a}_l \right], \tag{5}$$

where c is the speed of light, n_0 is the refractive index of the material, β_0 is the propagation constant in the individual waveguides, $\hat{a}_k^\dagger$ and $\hat{a}_k$ are the creation and annihilation operators in waveguide k, and $C_{k,l}$ is the coupling between waveguides k and l, where only nearest-neighbor coupling is assumed, that is, $l = k \pm 1$. The Heisenberg equations of motion in the comoving frame, describing the evolution of a single photon in the lattice, then take the following form:

$$i \frac{\mathrm{d}}{\mathrm{d}z} \hat{a}_k^\dagger(z) + \sum_l C_{k,l} \hat{a}_k^\dagger = 0, \tag{6}$$

with z as propagation distance in our optical setting, which acts as the evolution coordinate. Equation (6) can be formally integrated, such that one obtains the analytic solution for the $\hat{a}_k^\dagger(z)$:

$$\hat{a}_k^\dagger(z) = \sum_l U_{k,l}(z) \hat{a}_l^\dagger(0), \tag{7}$$

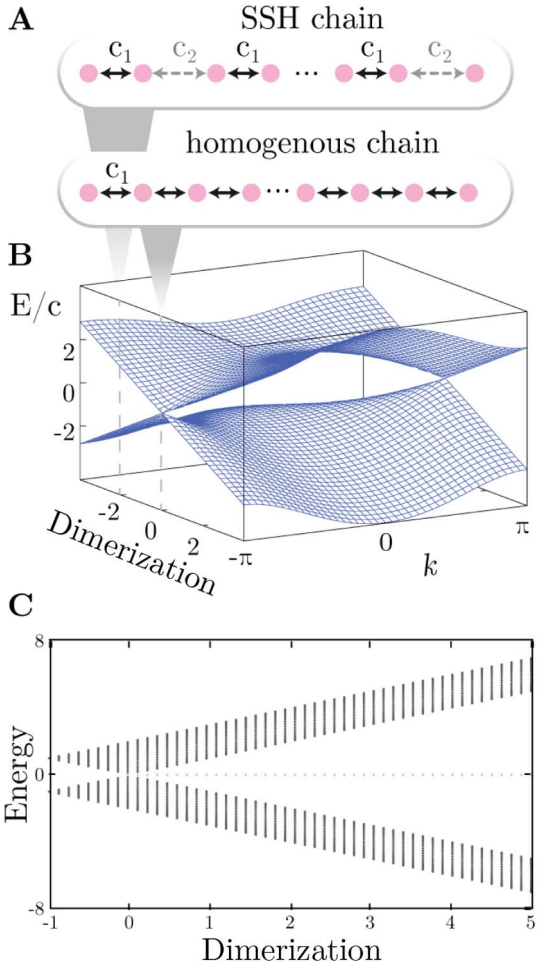

Fig. 1. Band structure of the Su–Schrieffer–Heeger model. (A) The SSH model describes a one-dimensional lattice with alternating nearest-neighbor couplings. For $d = 0$, the chain becomes homogenous. (B) Band structure of an infinite SSH chain. Any nonzero dimerization opens up a band gap. (C) Energy eigenvalues for a finite SSH chain terminated at a weak bond. A topological edge state of zero energy (marked light pink) resides in the band gap.

with the unitary propagation matrix $U_{k,l}(z)$ given by the expression

$$U_{k,l}(z) = (e^{izC})_{k,l}. \tag{8}$$

By its definition, $U_{k,l}(z)$ can be interpreted as the probability amplitude for a photon injected in guide l to be detected in channel k after propagation over the distance z. Hence, when a single photon is launched in waveguide k, the average photon number $\bar{n}_m(z)$ in channel m computes to

$$\bar{n}_m(z) = \langle \hat{a}_m^\dagger(z)\hat{a}_m(z)\rangle = |U_{m,k}(z)|^2. \tag{9}$$

When launching two photons in waveguides k and l, the average photon number is

$$\bar{n}_m(z) = |U_{m,k}(z)|^2 + |U_{m,l}(z)|^2. \tag{10}$$

This is the incoherent sum of the average photon numbers for single photon inputs in channels k and l. Hence, quantum path interference is never visible in the average photon number, regardless of the nature of the input state. In fact, the photon number evolves just like a classical intensity. In contrast, the two-photon correlation function $\Gamma_{k,l}$ of the photon outputs does depend on the input state and reveals this interference. This function is defined as

$$\Gamma_{m,n}(z) = \langle \hat{a}_m^\dagger(z)\hat{a}_n^\dagger(z)\hat{a}_n(z)\hat{a}_m(z)\rangle \tag{11}$$

and, hence, reads

$$\Gamma_{m,n}(z) = |U_{m,k}(z)U_{n,l}(z) + U_{m,l}(z)U_{n,k}(z)|^2. \tag{12}$$

When launching two indistinguishable photons into the lattice with one of the photons launched in channel k and the other in channel l, the function $\Gamma_{m,n}(z)$ relates to the joint probability of finding one photon in guide m and one in l at the same time via $P_{m,n} = \frac{1}{1+\delta_{m,n}}\Gamma_{m,n}$.

3. EXPERIMENTAL SETUP

For the fabrication of our waveguide lattices, we employ the femtosecond direct writing technology [49,50]; see Fig. 2(A) for a sketch of the setup. We inscribe the waveguides into transparent fused silica glass (Corning 7980), using ultrashort laser pulses ($\tau < 150$ fs, $\lambda = 800$ nm) that are focused 250 μm below the sample surface using a 20× microscope objective (NA ≈ 0.35). For a sketch of the writing setting, please refer to Fig. 2(A). Typical writing speeds achieved with a high-precision positioning system (Aerotech ANT180) are on the order of 100 mm/min, with a pulse energy of 500 nJ and a repetition rate of 100 kHz of the writing laser (Coherent Mira/Reg A). Such waveguides typically exhibit low propagation losses (<0.3 dB/cm) and support mode field diameters of 12 mm × 15 mm, yielding efficient coupling with 3 dB losses to standard single-mode fibers.

Along the length of the sample (150 mm), the fabricated structures comprise 41 waveguides and consist of three sections. The central section contains the actual lattice under investigation, that is, either an SSH lattice or a homogeneous lattice [see Fig. 2(B)]. The first and third sections are fanning structures that serve to match the fiber array spacing of 82 μm, with which the single photons are launched into and collected from the chip. The input fanning feeds the waveguides in which the photons are launched, whereas the output fanning collects the photons from a broader region in the lattice.

In our experiments, we employed a photon pair source at $\lambda = 815$ nm using a standard type I spontaneous parametric downconversion source with a visibility of 94%. A BiBO crystal is pumped by a 100 mW, 407.5 nm laser diode producing $|H\rangle$ polarized single-photon pairs collected by polarization

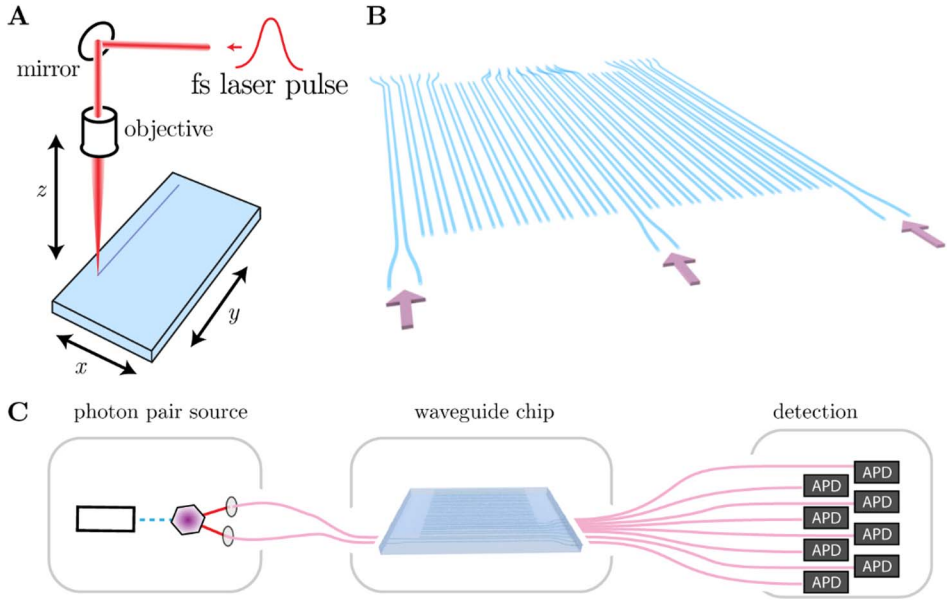

Fig. 2. Experimental setup. (A) Direct laser writing technique: femtosecond-laser pulses are focused into a moving glass sample, forming a waveguide trajectory. (B) Waveguide structure, consisting of an incoupling fanning, the actual SSH waveguide lattice with alternating couplings, and a fan-out. The lattice can be excited in the bulk, at the trivial and topological edge. (C) The full experimental setup consists of a spontaneous parametric down conversion (SPDC) photon pair source, fiber arrays that couple the photons into and out of the functional structure on the chip, and avalanche photodetectors.

maintaining fibers. Commercial V-groove fiber arrays with a pitch of 82 μm were used to couple the photons into the chip as well as to collect them at the output facet from the individual waveguides. Using high-NA multimode fibers in order to feed the photons to the respective avalanche photodiodes ensures low coupling losses at the output side of the chip. From the data of the photodiodes, the photon probability distribution at the output as well as the inter-channel correlations can be computed using a correlation device (Becker–Hickl) and standard software (LabView, MATLAB). Multiphoton events can be neglected, as for instance, when sending one photon from the downconversion pair into a chip the ratio of probabilities of two count events compared to single click events is 10^{-4} at the output of the system. Moreover, as the ratio of single clicks to zero-photon events was measured to be 0.03, the possibility of weak coherent input states can be excluded with high confidence.

4. RESULTS AND DISCUSSION

We start our experimental demonstration by characterizing the implemented lattices using a classical light source (cw laser excitation), which emulates a single-photon evolution. The results are summarized in Fig. 3, where simulations of the light evolution are shown in the left plots, and experimental light distribution for a propagation distance of $z = 10.47$ cm is shown on the right. When launching light at the topological edge, predominantly the topological edge state is populated, such that light stays mostly at this edge [see Fig. 3(A)]. There is some beating between the two outermost waveguides visible, because also some bulk modes are slightly populated. This changes when the waveguide at the trivial edge is excited. In this case, the absence of an edge state lets light diffract and penetrate into the bulk [Fig. 3(B)]. This behavior is similar to edge diffraction in homogeneous arrays, where likewise no edge state exists [Fig. 3(C)].

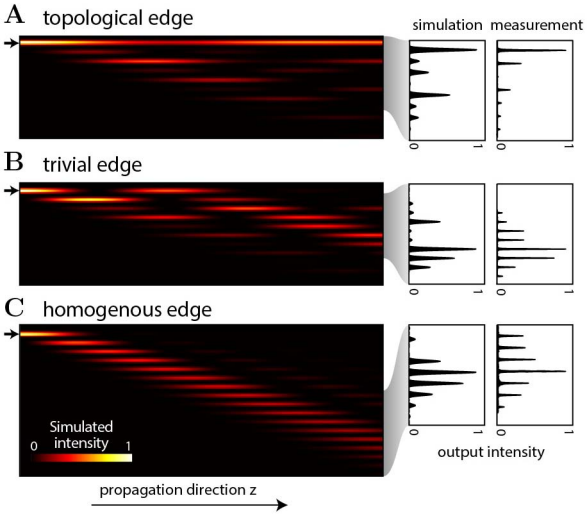

Fig. 3. Intensity propagation at the lattice edges. The figures on the left show the simulated intensity evolution along the z axis when the edge is excited, and on the right the measured output intensities at the end of the lattice are depicted. (A) At the topological edge, light propagates from the edge into the bulk, in contrast to (B) the trivial edge, where part of the edge state is excited and intensity remains in the edge waveguide. (C) In the homogenous array, there is no edge state and the intensity is transported into the bulk ballistically.

When launching two indistinguishable photons into the lattice at different positions, the correlation function $\Gamma_{m,n}(z = 10.47\ \text{cm})$ can be retrieved from coincidence measurements between the individual detectors. These coincidence measurements reveal the probability of finding one photon at waveguide n when the other is detected in waveguide m. Note that the avalanche photodetectors employed in our experiments cannot distinguish photon numbers, precluding measurements of the main diagonal elements of the correlation matrix. We start by probing the topological edge and launch one photon directly into the edge waveguide. In this vein, it efficiently populates the topological state, whereas the other photon is launched into the waveguide next to it and predominantly populates bulk states. The corresponding correlation patterns are shown in Fig. 4(A), revealing a significant chance of detecting one of the photons directly in the edge waveguide, whereas the other penetrated into the bulk. As a result, the chance of finding both photons in the edge waveguides is low at the end of the sample, despite the fact that they were launched in close proximity to one another. Moreover, there is a certain chance that both photons penetrate into the bulk together, although one photon still mainly populates the topological edge state. Exciting the edge waveguide means exciting a superposition of the edge state and bound states, that evolve into the bulk. The interference with the second photon which does not populate the edge state shows in the correlation measurement. This picture changes considerably when the photons are launched into the trivial edge [Fig. 4(C)]. In this case the photons tend to co-propagate, and the chance of finding them close together inside the bulk is significant. In contrast, the probability that one or both photons remain at the edge is negligible. The latter case is reminiscent of both photons being launched in adjacent waveguides in the bulk of the lattice [Fig. 4(B)]. In line with the inherent bunching behavior of indistinguishable photons, they tend to stay close to each other during their evolution.

We compare this to the two-photon correlations in a homogeneous lattice, where all hoppings between the waveguides are identical (the dimerization is zero). In this case, the photons inevitably exhibit bunching and are found with high probability close to each other, irrespective of whether they were launched into the bulk of the lattice [Fig. 4(G), first measured in Ref. [40]) or close to the edge of the lattice (Fig. 4(H)], without being affected by the topology of the lattice.

Another important measure for characterizing the particle evolution in the lattice is the inter-particle distance probability $g(\Delta)$ as a function of the distance Δ, which can be retrieved directly from the two-particle correlation function by [51,52]

$$g(\Delta) = \sum_m \Gamma_{m,m+\Delta}. \tag{13}$$

Figure 5(A) shows the results for the topological edge of the SSH lattice, retrieved from the correlation matrices plotted in Fig. 4. Notably, the probability of finding the photons close to each other is approximately the same as finding the

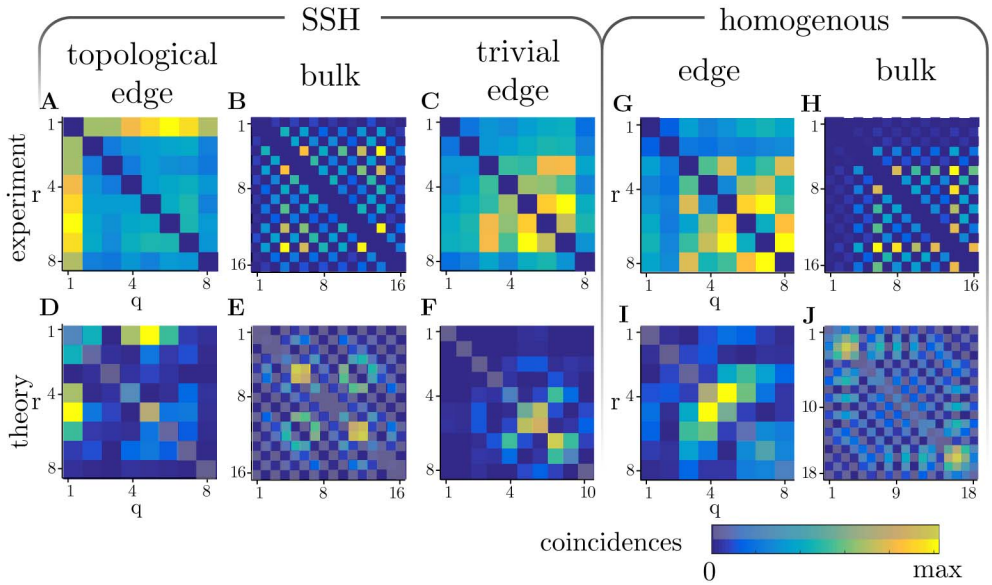

Fig. 4. Correlations in the SSH lattice. Two indistinguishable photons are launched into neighboring sites of a lattice at the topological edge, trivial edge, and bulk. The coincidence counts after the quantum walk are shown in the upper row, and the corresponding theory is depicted below. For comparison, a homogenous lattice is investigated on the right. On the topological edge, the photons tend to remain in the edge state, which clearly shows in the measurement. The diagonal elements of the correlation matrices are not accessible without photon number resolution and are therefore masked gray in the simulations.

photons apart. In other words, although only one photon populates mostly the edge state and the second one could—in principle—freely escape into the bulk, the chance of having the photons close together is essentially the same as finding them far away from each other. This is clearly a surprising feature of the topological edge: the entangled two-photon state after propagating through the lattice is highly complex, with approximately equal probability for various distances between the two photons. This is very different when the photons are launched at the trivial edge of the SSH lattice. In this case, the inter-particle distance probability [retrieved from the correlation matrices shown in Fig. 4(B)] is largest for small distances and rapidly decreases for increasing distance as plotted in Fig. 5(B). In other words, the photons indeed stay close together while they penetrate the bulk of the system, which indeed underlines their bunching behavior.

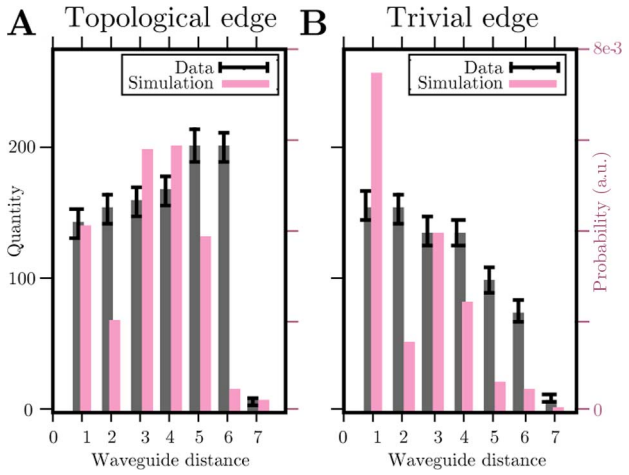

Fig. 5. Inter-particle distance. Histogram for the distance between the photon pairs detected in the quantum walk (see Fig. 4). At the topological edge, one of the photons tends to remain in the edge state, leading to a higher inter-particle distance than at the trivial edge, where the photons tend to remain in close proximity. Note that due to the use of avalanche photodiodes as detectors, the cases in which both photons arrive in the same channel are systematically inaccessible in the experiments, preventing a normalization of the inter-particle distance distributions. Further deviations can be attributed to imperfections of the synthesized input state due to the limited accuracy of the polarization alignment between the two injection fibers.

5. CONCLUSION AND OUTLOOK

In our work, we observed two-particle quantum correlations of indistinguishable photons at the edge and in the bulk of an SSH waveguide lattice and compared them to the correlations in a homogeneous lattice. We find that, whereas at the trivial edge in the SSH lattice the bunching behavior of the indistinguishable photons remains unchanged, the bunching is significantly distorted at the topological edge. Although one photon remains at the edge with high probability and the other mostly penetrates into the bulk, the joint probability of finding the photons close to each other after propagating through the sample has approximately the same magnitude as the probability that the photons leave the sample far away from each other. Therefore, the existence of the edge state at the topological edge in the SSH model has a significant influence on the quantum interference of indistinguishable photons.

Our work sheds new light on the quantum features of topologically nontrivial lattices and may help to find new applications in preparing and transmitting complex quantum states. There are several questions that can be asked. What behavior

can be observed in higher-dimensional topological systems, and in particular higher-order topological insulators? What is the impact of topological edge states on states with larger number of photons? And what happens in the case of non-Hermiticity, in particular parity-time symmetry? These and related problems are now in reach to be explored experimentally.

APPENDIX A

1. Photon Pair Generation

We generate indistinguishable photon pairs through type I spontaneous parametric downconversion of 407.5 nm laser light on a BiBO crystal. For characterization of the source, the photon pairs are coupled into a fiber 50/50 beamsplitter to perform a Hong–Ou–Mandel experiment. By tuning the length of the collection arm for one of the photons, the time delay between the photons can be adjusted, leading to the coincidence data depicted in Fig. 6. The recorded Hong–Ou–Mandel dip was fitted with a Gaussian curve, retrieving a visibility of 94% ± 2%.

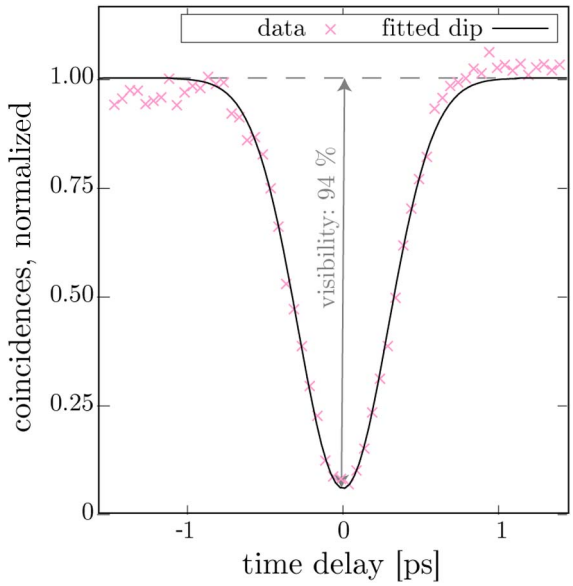

Fig. 6. Hong–Ou–Mandel dip of the photon pair source. The retrieved coincidence counts (pink) were fitted with a Gaussian function (black), characterizing the visibility at 94% ± 2%.

2. Additional Propagation Simulations

In the experiment, indistinguishable photons were launched into the edge waveguides and the corresponding neighboring sites. Although the evolution of the photon pairs deviates from the purely classical case, the simulations of classical light launched into the edge neighboring waveguides might give some intuition about the dynamics in the system.

In Fig. 7 these evolutions are depicted. We obtain the images using a Crank–Nicholson propagation with Eq. (6), obtaining the propagated states $a(z)$. Using Eq. (10) we calculate the photon numbers in the waveguides and using Eq. (11) we simulate the correlation matrices.

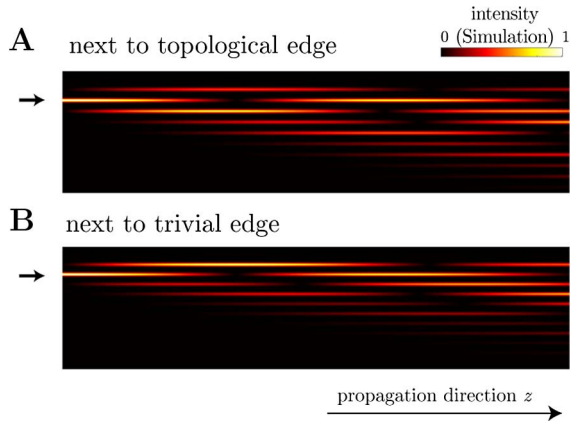

Fig. 7. Additional simulations of intensity propagation for classical light launched into the edge neighboring waveguides.

Funding. Alfried Krupp von Bohlen und Halbach-Stiftung; Deutsche Forschungsgemeinschaft (BL 574/13-1, SCHE 612/6-1, SZ 276/12-1, SZ 276/15-1, SZ 276/20-1).

Acknowledgment. The authors would like to thank C. Otto for preparing the high-quality fused silica samples employed in this work.

Disclosures. The authors declare no conflicts of interest.

REFERENCES

1. L. Lu, J. D. Joannopoulos, and M. Soljačić, "Topological photonics," Nat. Photonics **8**, 821–829 (2014).
2. T. Ozawa, H. M. Price, A. Amo, N. Goldman, M. Hafezi, L. Lu, M. C. Rechtsman, D. Schuster, J. Simon, O. Zilberberg, and I. Carusotto, "Topological photonics," Rev. Mod. Phys. **91**, 015006 (2019).
3. C. L. Kane and E. J. Mele, "Z2 topological order and the quantum spin Hall effect," Phys. Rev. Lett. **95**, 146802 (2005).
4. B. A. Bernevig and S. C. Zhang, "Quantum spin Hall effect," Phys. Rev. Lett. **96**, 106802 (2006).
5. M. König, S. Wiedmann, C. Brüne, A. Roth, H. Buhmann, L. W. Molenkamp, X. L. Qi, and S. C. Zhang, "Quantum spin hall insulator state in HgTe quantum wells," Science **318**, 766–770 (2007).
6. D. Hsieh, D. Qian, L. Wray, Y. Xia, Y. S. Hor, R. J. Cava, and M. Z. Hasan, "A topological Dirac insulator in a quantum spin Hall phase," Nature **452**, 970–974 (2008).
7. S. Raghu and F. D. M. Haldane, "Analogs of quantum-Hall-effect edge states in photonic crystals," Phys. Rev. A **78**, 033834 (2008).
8. F. D. M. Haldane and S. Raghu, "Possible realization of directional optical waveguides in photonic crystals with broken time-reversal symmetry," Phys. Rev. Lett. **100**, 013904 (2008).
9. Z. Wang, Y. D. Chong, J. D. Joannopoulos, and M. Soljačić, "Reflection-free one-way edge modes in a gyromagnetic photonic crystal," Phys. Rev. Lett. **100**, 013905 (2008).
10. Z. Wang, Y. Chong, J. D. Joannopoulos, and M. Soljačić, "Observation of unidirectional backscattering-immune topological electromagnetic states," Nature **461**, 772–775 (2009).
11. M. C. Rechtsman, J. M. Zeuner, Y. Plotnik, Y. Lumer, D. Podolsky, F. Dreisow, S. Nolte, M. Segev, and A. Szameit, "Photonic Floquet topological insulators," Nature **496**, 196–200 (2013).
12. M. Hafezi, S. Mittal, J. Fan, A. Migdall, and J. M. Taylor, "Imaging topological edge states in silicon photonics," Nat. Photonics **7**, 1001–1005 (2013).
13. L. J. Maczewsky, J. M. Zeuner, S. Nolte, and A. Szameit, "Observation of photonic anomalous Floquet topological insulators," Nat. Commun. **8**, 13756 (2017).

14. S. Mukherjee, A. Spracklen, M. Valiente, E. Andersson, P. Öhberg, N. Goldman, and R. R. Thomson, "Experimental observation of anomalous topological edge modes in a slowly driven photonic lattice," Nat. Commun. **8**, 13918 (2017).
15. O. Zilberberg, S. Huang, J. Guglielmon, M. Wang, K. P. Chen, Y. E. Kraus, and M. C. Rechtsman, "Photonic topological boundary pumping as a probe of 4D quantum Hall physics," Nature **553**, 59–62 (2018).
16. J. Noh, S. Huang, D. Leykam, Y. D. Chong, K. P. Chen, and M. C. Rechtsman, "Experimental observation of optical Weyl points and Fermi arc-like surface states," Nat. Phys. **13**, 611–617 (2017).
17. S. Stützer, Y. Plotnik, Y. Lumer, P. Titum, N. H. Lindner, M. Segev, M. C. Rechtsman, and A. Szameit, "Photonic topological Anderson insulators," Nature **560**, 461–465 (2018).
18. E. Lustig, S. Weimann, Y. Plotnik, Y. Lumer, M. A. Bandres, A. Szameit, and M. Segev, "Photonic topological insulator in synthetic dimensions," Nature **567**, 356–360 (2019).
19. S. Weimann, M. Kremer, Y. Plotnik, Y. Lumer, S. Nolte, K. G. Makris, M. Segev, M. C. Rechtsman, and A. Szameit, "Topologically protected bound states in photonic parity–time-symmetric crystals," Nat. Mater. **16**, 433–438 (2017).
20. J. M. Zeuner, M. C. Rechtsman, Y. Plotnik, Y. Lumer, S. Nolte, M. S. Rudner, M. Segev, and A. Szameit, "Observation of a topological transition in the bulk of a non-Hermitian system," Phys. Rev. Lett. **115**, 040402 (2015).
21. S. Barik, A. Karasahin, C. Flower, T. Cai, H. Miyake, W. DeGottardi, M. Hafezi, and E. Waks, "A topological quantum optics interface," Science **359**, 666–668 (2018).
22. A. Blanco-Redondo, B. Bell, D. Oren, B. J. Eggleton, and M. Segev, "Topological protection of biphoton states," Science **362**, 568–571 (2018).
23. W. P. Su, J. R. Schrieffer, and A. J. Heeger, "Solitons in polyacetylene," Phys. Rev. Lett. **42**, 1698–1701 (1979).
24. A. P. Schnyder, S. Ryu, A. Furusaki, and A. W. W. Ludwig, "Classification of topological insulators and superconductors in three spatial dimensions," Phys. Rev. B **78**, 195125 (2008).
25. N. Malkova, I. Hromada, X. Wang, G. Bryant, and Z. Chen, "Observation of optical Shockley-like surface states in photonic superlattices," Opt. Lett. **34**, 1633–1635 (2009).
26. C. Jürß and D. Bauer, "High-harmonic generation in Su-Schrieffer-Heeger chains," Phys. Rev. B **99**, 195428 (2019).
27. V. Dal Lago, M. Atala, and L. E. F. Foa Torres, "Floquet topological transitions in a driven one-dimensional topological insulator," Phys. Rev. A **92**, 023624 (2015).
28. Z. Fedorova, C. Jörg, C. Dauer, F. Letscher, M. Fleischhauer, S. Eggert, S. Linden, and G. von Freymann, "Limits of topological protection under local periodic driving," Light Sci. Appl. **8**, 1 (2019).
29. E. J. Meier, F. A. An, and B. Gadway, "Observation of the topological soliton state in the Su-Schrieffer-Heeger model," Nat. Commun. **7**, 13986 (2016).
30. M. A. Miri, M. Heinrich, R. El-Ganainy, and D. N. Christodoulides, "Supersymmetric optical structures," Phys. Rev. Lett. **110**, 233902 (2013).
31. G. Queraltó, M. Kremer, L. J. Maczewsky, M. Heinrich, J. Mompart, V. Ahufinger, and A. Szameit, "Topological state engineering via supersymmetric transformations," Commun. Phys. **3**, 49 (2020).
32. M. C. Rechtsman, Y. Lumer, Y. Plotnik, A. Perez-Leija, A. Szameit, and M. Segev, "Topological protection of photonic path entanglement," Optica **3**, 925–930 (2016).
33. S. Mittal, V. V. Orre, and M. Hafezi, "Topologically robust transport of entangled photons in a 2D photonic system," Opt. Express **24**, 15631–15641 (2016).
34. S. Mittal, E. A. Goldschmidt, and M. Hafezi, "A topological source of quantum light," Nature **561**, 502–506 (2018).
35. M. Wang, C. Doyle, B. Bell, M. J. Collins, E. Magi, B. J. Eggleton, M. Segev, and A. Blanco-Redondo, "Topologically protected entangled photonic states," Nanophotonics **8**, 1327–1335 (2019).
36. J. L. Tambasco, G. Corrielli, R. J. Chapman, A. Crespi, O. Zilberberg, R. Osellame, and A. Peruzzo, "Quantum interference of topological states of light," Sci. Adv. **4**, eaat3187 (2018).
37. Y. Aharonov, L. Davidovich, and N. Zagury, "Quantum random walks," Phys. Rev. A **48**, 1687–1690 (1993).
38. H. B. Perets, Y. Lahini, F. Pozzi, M. Sorel, R. Morandotti, and Y. Silberberg, "Realization of quantum walks with negligible decoherence in waveguide lattices," Phys. Rev. Lett. **100**, 170506 (2008).
39. Y. Bromberg, Y. Lahini, R. Morandotti, and Y. Silberberg, "Quantum and classical correlations in waveguide lattices," Phys. Rev. Lett. **102**, 253904 (2009).
40. A. Peruzzo, M. Lobino, J. C. F. Matthews, N. Matsuda, A. Politi, K. Poulios, X.-Q. Zhou, Y. Lahini, N. Ismail, K. Wörhoff, Y. Bromberg, Y. Silberberg, M. G. Thompson, and J. L. O'Brien, "Quantum walks of correlated photons," Science **329**, 1500–1503 (2010).
41. K. Poulios, R. Keil, D. Fry, J. D. A. Meinecke, J. C. F. Matthews, A. Politi, M. Lobino, M. Gräfe, M. Heinrich, S. Nolte, A. Szameit, and J. L. O'Brien, "Quantum walks of correlated photon pairs in two-dimensional waveguide arrays," Phys. Rev. Lett. **112**, 143604 (2014).
42. M. A. Broome, A. Fedrizzi, S. Rahimi-Keshari, J. Dove, S. Aaronson, T. C. Ralph, and A. G. White, "Photonic boson sampling in a tunable circuit," Science **339**, 794–798 (2013).
43. J. B. Spring, B. J. Metcalf, P. C. Humphreys, W. S. Kolthammer, X. M. Jin, M. Barbieri, A. Datta, N. Thomas-Peter, N. K. Langford, D. Kundys, J. C. Gates, B. J. Smith, P. G. R. Smith, and I. A. Walmsley, "Boson sampling on a photonic chip," Science **339**, 798–801 (2013).
44. A. Crespi, R. Osellame, R. Ramponi, D. J. Brod, E. F. Galvão, N. Spagnolo, C. Vitelli, E. Maiorino, P. Mataloni, and F. Sciarrino, "Integrated multimode interferometers with arbitrary designs for photonic boson sampling," Nat. Photonics **7**, 545–549 (2013).
45. M. Tillmann, B. Dakić, R. Heilmann, S. Nolte, A. Szameit, and P. Walther, "Experimental boson sampling," Nat. Photonics **7**, 540–544 (2013).
46. N. Malkova, I. Hromada, X. Wang, G. Bryant, and Z. Chen, "Transition between Tamm-like and Shockley-like surface states in optically induced photonic superlattices," Phys. Rev. A **80**, 043806 (2009).
47. F. L. J. Vos, D. P. Aalberts, and W. van Saarloos, "Su-Schrieffer-Heeger model applied to chains of finite length," Phys. Rev. B **53**, 14922–14928 (1996).
48. M. Gräfe, R. Heilmann, R. Keil, T. Eichelkraut, M. Heinrich, S. Nolte, and A. Szameit, "Correlations of indistinguishable particles in non-Hermitian lattices," New J. Phys. **15**, 033008 (2013).
49. K. M. Davis, K. Miura, N. Sugimoto, and K. Hirao, "Writing waveguides in glass with a femtosecond laser," Opt. Lett. **21**, 1729–1731 (1996).
50. A. Szameit and S. Nolte, "Discrete optics in femtosecond-laser-written photonic structures," J. Phys. B **43**, 163001 (2010).
51. Y. Lahini, Y. Bromberg, D. N. Christodoulides, and Y. Silberberg, "Quantum correlations in two-particle Anderson localization," Phys. Rev. Lett. **105**, 163905 (2010).
52. M. Lebugle, M. Gräfe, R. Heilmann, A. Perez-Leija, S. Nolte, and A. Szameit, "Experimental observation of N00N state Bloch oscillations," Nat. Commun. **6**, 8273 (2015).